Egyptian Journal of Radiology and Nuclear Medicine

CASE REPORT

Open Access

Case series on neuroimaging spectrum of Wilson's disease: knowing the known and the uncommonly known

Kunal Patel[1], Aanchal Bhayana[1*], Neha Bagri[1] and Amita Malik[1]

Abstract

Background Wilson's disease is an inherited disease characterized by impaired copper metabolism that causes damage to many organs, including the brain. Patients having neurological involvement usually present with varied neuropsychiatric symptoms. Magnetic resonance imaging (MRI) Brain plays an indispensable role in identifying the structural involvement in these patients, aiding in early accurate diagnosis and timely management. Typically, basal ganglia, thalami and brainstem are involved, with bright claustrum sign, face of giant panda sign and miniature panda signs on MRI.

Conclusions Having knowledge about the commonly encountered and known MRI brain findings in Wilson's disease are essential in aiding accurate diagnosis and initiating early management. However, identifying the Atypical MRI brain characteristics is all the more imperative and should be considered in patients with prolonged or severe disease or in patients with rapid clinical progression and in patients showing poor response to treatment.

Keywords Case series, Wilson's disease, MRI Brain, Bright claustrum sign, Face of giant panda sign, Miniature panda sign, White matter changes, Subcortical cysts, Middle cerebellar peduncle

Background

Wilson's disease (WD), also known as hepatolenticular degeneration is an autosomal recessive disorder, caused by mutation of the ATP7B gene, located on chromosome 13q14.3 [2]. This mutation results in impaired copper metabolism and excretion, with failure to incorporate copper into ceruloplasmin, leading to accumulation of free toxic copper in various organs predominantly brain, liver, cornea and kidneys triggering organ damage [2]. Patients having neurological involvement usually present with varied neuropsychiatric manifestations [3]. MRI Brain plays an indispensible role in identifying the structural involvement in such patients, aiding in early accurate diagnosis, thereby guiding clinicians towards appropriate management. Though several reports on the typical neuroradiological findings in WD involving basal ganglia, thalami, and brainstem with characteristic giant panda appearance have been published from both the Indian and Western investigators, there are not many reports on the atypical brain MRI findings, especially from Indian literature. The atypical brain features like involvement of middle cerebellar peduncles and white matter changes are an unfamiliar sight in WD, posing a diagnostic dilemma [1–19].

We hereby report spectrum of neuroimaging features of WD in four adolescent patients with diverse neurological symptoms. Moreover, the uniqueness of our series is that, in two of our cases atypical brain MRI features were observed, one depicting extensive white matter involvement with cystic changes and the other showing striking involvement of superior and middle cerebellar peduncles.

*Correspondence:
Aanchal Bhayana
aanchalbhayana@gmail.com
[1] Department of Radiodiagnosis and Intervention Radiology, VMMC and Safdarjung Hospital, Room No 15, H Block, New Delhi 110029, India

The aim of this report was thus to demystify the neuroimaging spectrum of newly diagnosed cases of Wilson's disease, with early identification of atypical and uncommonly observed features, especially white matter changes, over and above the known typical features, that may be red flag signs of either a prolonged or severe disease or rapid clinical progression and poor response to treatment.

Case presentation

We report spectrum of neuroimaging features of newly diagnosed Wilson's disease in four adolescent patients on MRI Brain. Non-contrast MRI Brain was performed in all four patients, on 3 T MR machine (GE discovery MR750 W 3 T) using head and neck coil and following MRI sequences were included—3D FSPGR, T2W, FLAIR, DWI and SWAN. The images were reviewed by two radiologists, with an experience of 12 years and 3 years respectively.

Case 1

An 18 years old female patient with complaints of involuntary movement of bilateral upper limbs and history of multiple falls in dark since 1 year. On examination, broad based gait and dysdiadochokinesia was observed. No significant family history was noted. Ophthalmologic examination revealed bilateral Kayser–Fleischer (KF) rings. Serum copper and ceruloplasmin levels were 76.5 µg/dL (118–302 µg/dL) and 0.03 g/L (0.25–0.63 g/L), respectively. On MRI Brain, symmetrical T2/FLAIR hyperintensity was seen in bilateral caudate, putamen and thalami with bright claustrum sign (Fig. 1A). Symmetrical T2 hypointensity was noted in bilateral globus pallidi with blooming on SWI (Fig. 1A, B). T2 weighted image showed face of giant panda sign and face of miniature panda sign in the midbrain and pons respectively (Fig. 1C, D) Based on clinic-radiological features and biochemical investigations, a diagnosis of Wilson's disease with typical MRI Brain features was made. Following this, the patient was started on Zinc 50 mg TDS and penicillamine 500 mg BD with 25 mg of pyridoxine. Clinically the patient showed neurological improvement, however follow up imaging was not performed.

Case 2

An 18 years old male patient presented with complaints of difficulty in walking and history of recurrent falls for last 2 months, difficulty in speaking and swallowing for last 1 month. Clinical examination revealed generalized hypertonia across all joints, short stepped gait and cog wheel rigidity. There was no similar family history. Ophthalmologic examination revealed bilateral Kayser–Fleischer rings. Ceruloplasmin and 24 h urinary copper levels were obtained which were 42 mg/dl (20–60 mg/dl) and 322 ug/24 h (3–50 ug/24 h) respectively. On MRI Brain, symmetrical T2/FLAIR hyperintensity was noted in bilateral caudate, peripheral parts of bilateral putamen and lateral parts of bilateral thalami (Fig. 2A). T2 hypointensity was seen in the central parts of bilateral putamen and bilateral globus pallidi, with areas of blooming on SWI (Fig. 2B, C). No corresponding T1 weighted changes were noted in the basal ganglia (Fig. 2D). Based on clinic-radiological features and biochemical investigations, a diagnosis of Wilson's disease with typical MRI Brain features was made. Following the diagnosis, the patient's treatment was initiated with Zinc 50 mg TDS and penicillamine 500 mg BD with 25 mg of pyridoxine. Following this treatment, the patient showed neurological improvement and was discharged.

Case 3

A 16 years old female patient with complaints of involuntary movement of right hand followed by left hand, progressive in nature since last 4 months. On examination, wing beating tremors and dysarthria were elicited. No similar family history was obtained. Ophthalmologic examination revealed bilateral Kayser–Fleischer rings (Fig. 3A, B). Serum ceruloplasmin and 24-h urinary copper levels were obtained which were 9 mg/dl (22–60 mg/dl) and 19.20 ug/24 h (15–70 ug/24 h) respectively. MRI Brain revealed T2/FLAIR symmetrical hyperintensity in bilateral putamen with thin T2 hyperintensity in claustrum (bright claustrum sign) and bilateral thalami (Fig. 4A, B). Symmetrical T2 hypointensity was noted in bilateral globus pallidi, with areas of blooming on SWI (Fig. 4A, C). Further, T2 hyperintensity was noted in tegmentum of the midbrain, with hypointense red nuclei, hypointense superior colliculi and hypointense pars reticulata of substantia nigra, depicting "face of giant panda sign" (Fig. 4D). T2 hyperintensity was also seen in the dorsal pontine tegmentum with hypointense medial longitudinal fasciculus and central tegmental tract, hyperintense aqueduct opening into fourth ventricle and hyperintense superior cerebellar peduncles, depicting "face of miniature panda sign" (Fig. 4E). Atypically, symmetrical T2 hyperintensity was observed in bilateral middle cerebellar peduncles (Fig. 4F). Based on clinic-radiological features and biochemical investigations, a diagnosis of Wilson's disease with atypical MRI Brain features was made. Subsequently, the patient was started on Zinc 50 mg TDS and penicillamine 500 mg BD with 25 mg of pyridoxine, however the patient showed no clinical improvement even after 6 months of starting the treatment. No follow up imaging was done.

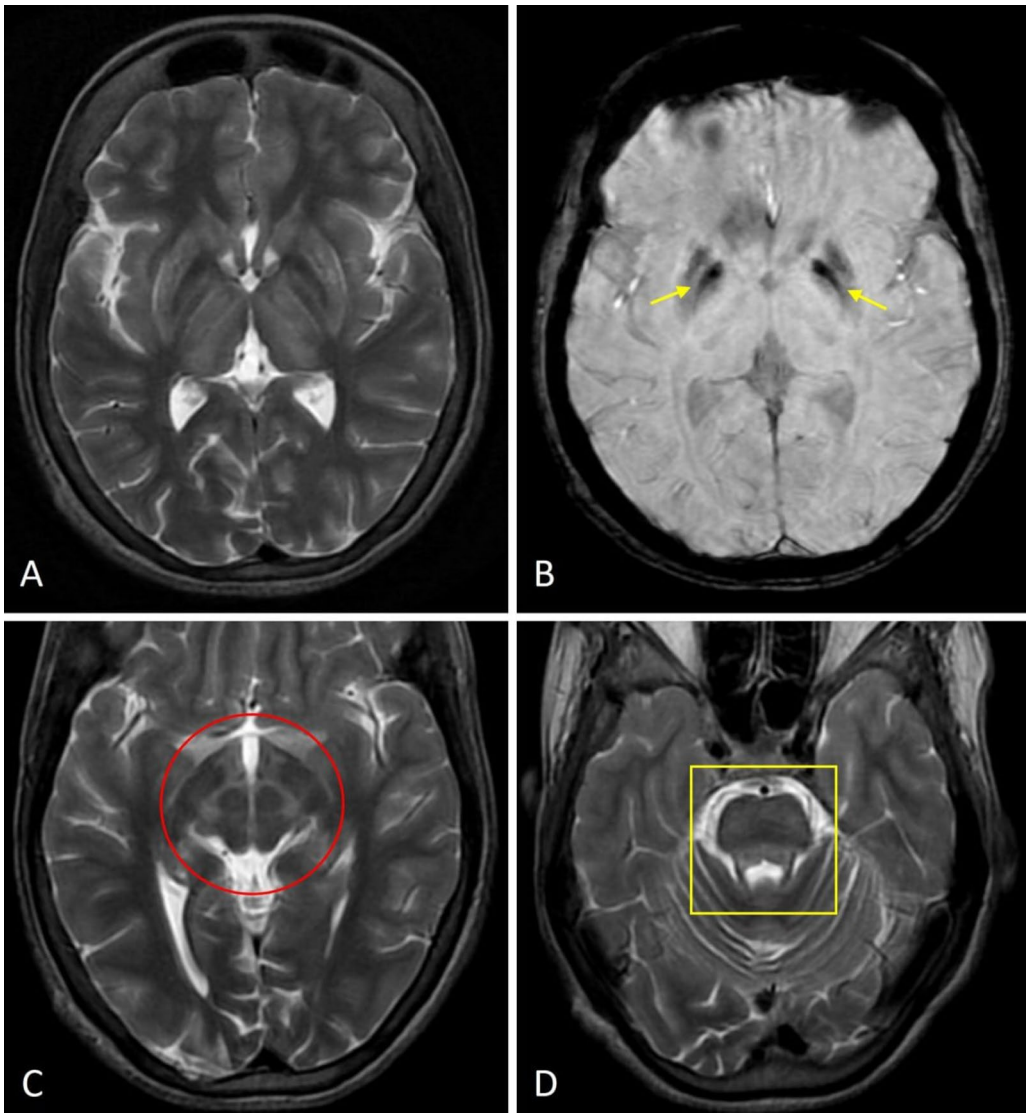

Fig. 1 Axial T2 weighted MR image (**A**) shows symmetrical hyperintensity in bilateral caudate, putamen and thalami with bright claustrum sign. Symmetrical hypointensity is noted in bilateral globus pallidi. Axial SWAN MR image (**B**) shows symmetrical areas of blooming in bilateral globus pallidi (yellow arrows). Axial T2 weighted MR image at the level of midbrain (**C**) and at the level of pons (**D**) shows "face of giant panda sign" (red circle) and "face of miniature panda sign" (yellow box) respectively

Case 4

A 13 years old male patient presented with involuntary movement of bilateral upper limbs followed by lower limbs for last 3 months, with abnormal behaviour and abnormal facial expressions for last 15 days. No similar family history was noted. Ophthalmologic examination revealed bilateral Kayser–Fleischer rings (Fig. 5A). Serum ceruloplasmin levels were 7 mg/dl (20–60 mg/dl). On MRI Brain, symmetrical T2/FLAIR hyperintensity was noted in bilateral caudate, putamen, posterior limb of internal capsule, bilateral thalami and bilateral claustrum (Fig. 5B). Symmetrical T2 hypointensity was noted in bilateral globus pallidi with blooming on SWI (Fig. 5B, C). Midbrain and pontine tegmentum showed face of giant panda sign and face of miniature panda sign respectively on T2 weighted images (Fig. 5D, E). Additionally, T2/FLAIR bilateral, symmetrical, confluent white matter hyperintensities were seen in the frontal, parietal and temporal lobes (Fig. 6A–D). Also, bilaterally symmetrical T2 hyperintense and FLAIR hypointense subcortical cystic areas were observed in bilateral frontal and temporal lobes (Fig. 6A–D). Diffusion weighted images (DWI) showed focal areas of diffusion restriction in bilateral frontal and parietal white matter (Fig. 6E, F). Moreover,

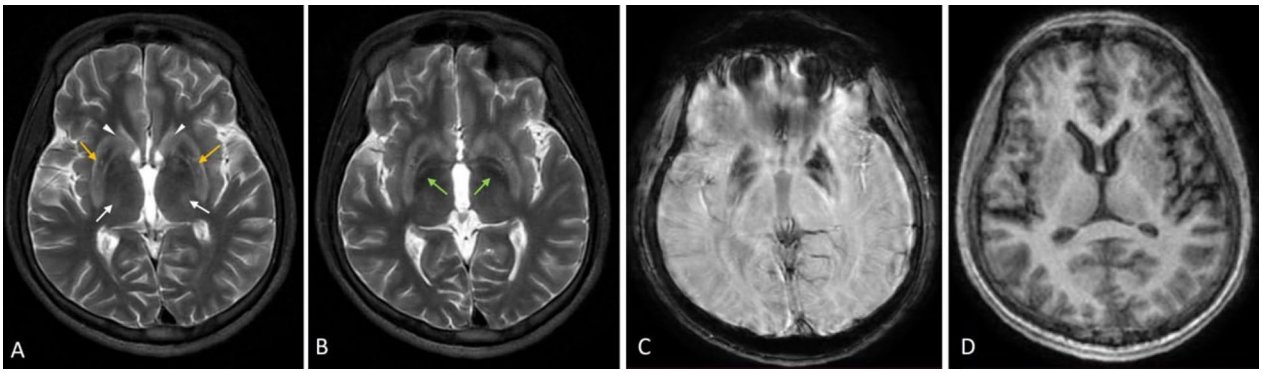

Fig. 2 Axial T2 weighted MR image (**A**) shows symmetrical hyperintensity in bilateral caudate (white arrow heads), peripheral parts of bilateral putamen and lateral parts of bilateral thalami (white arrows). Hypointenity is seen involving the central parts of bilateral putamen (orange arrows). Axial T2 weighted MR image (**B**) shows symmetrical hypointensity in bilateral globus pallidi (green arrows). Axial SWAN MR image (**C**) shows symmetrical areas of blooming in bilateral globus pallidi and central parts of bilateral putamen. Axial T1 weighted MR image (D) shows no obvious abnormal hyperintensities in bilateral basal ganglia

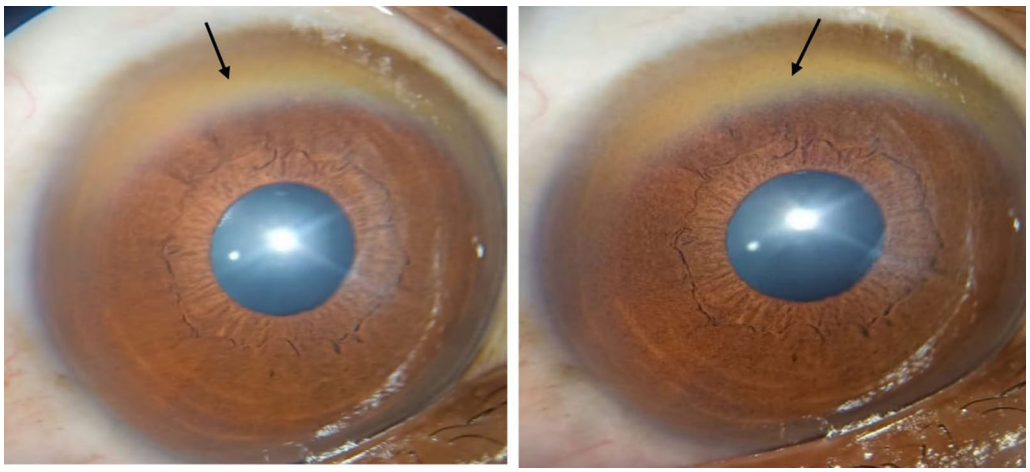

Fig. 3 Slit lamp examination of both eyes showing golden to brown coloured Kayser-Fleisher rings at the superior aspect of bilateral cornea (black arrows)

cerebral atrophy in the form of mildly prominent bilateral lateral ventricles was also noted (Fig. 6G, H). Based on these radiological features and clinico-biochemical evaluation, a diagnosis of Wilson's disease with atypical MRI Brain features was made. Following the diagnosis, the patient was immediately started on Zinc 50 mg TDS and penicillamine 500 mg BD with 25 mg of pyridoxine. However, the patient showed poor response to treatment, with no significant clinical improvement, likely attributed to the marked white matter changes and cystic areas.

Discussion

Wilson's disease (WD) is an autosomal recessive disorder, resulting from mutations in ATP7B gene on chromosome 13, which encodes a transmembrane copper transporting ATPase expressed on hepatocyte membrane facilitating intrahepatic combination of copper and apoceruloplasmin into ceruloplasmin. This process is responsible for elimination of nearly 90% of circulating copper in normal individuals. Thus, in WD, there occurs a decrease in circulating ceruloplasmin and copper accumulation in hepatocytes. This excess hepatic copper causes toxic injury, either by facilitating free radical formation or by binding to sulfhydryl groups of cellular proteins or by displacing other metals from hepatic metalloenzymes [2]. Ultimately, the excessive free copper accumulates in various tissues like brain, cornea and kidneys causing organ damage [2].

The age at onset of WD ranges from 6 to 40 years of age (average age being 11.4 years) [3]. Its clinical presentation is extremely variable. Some patients present with acute or chronic liver disease. Others present with predominant neuropsychiatric symptoms with movement disorders like dystonia, incoordination, and tremors,

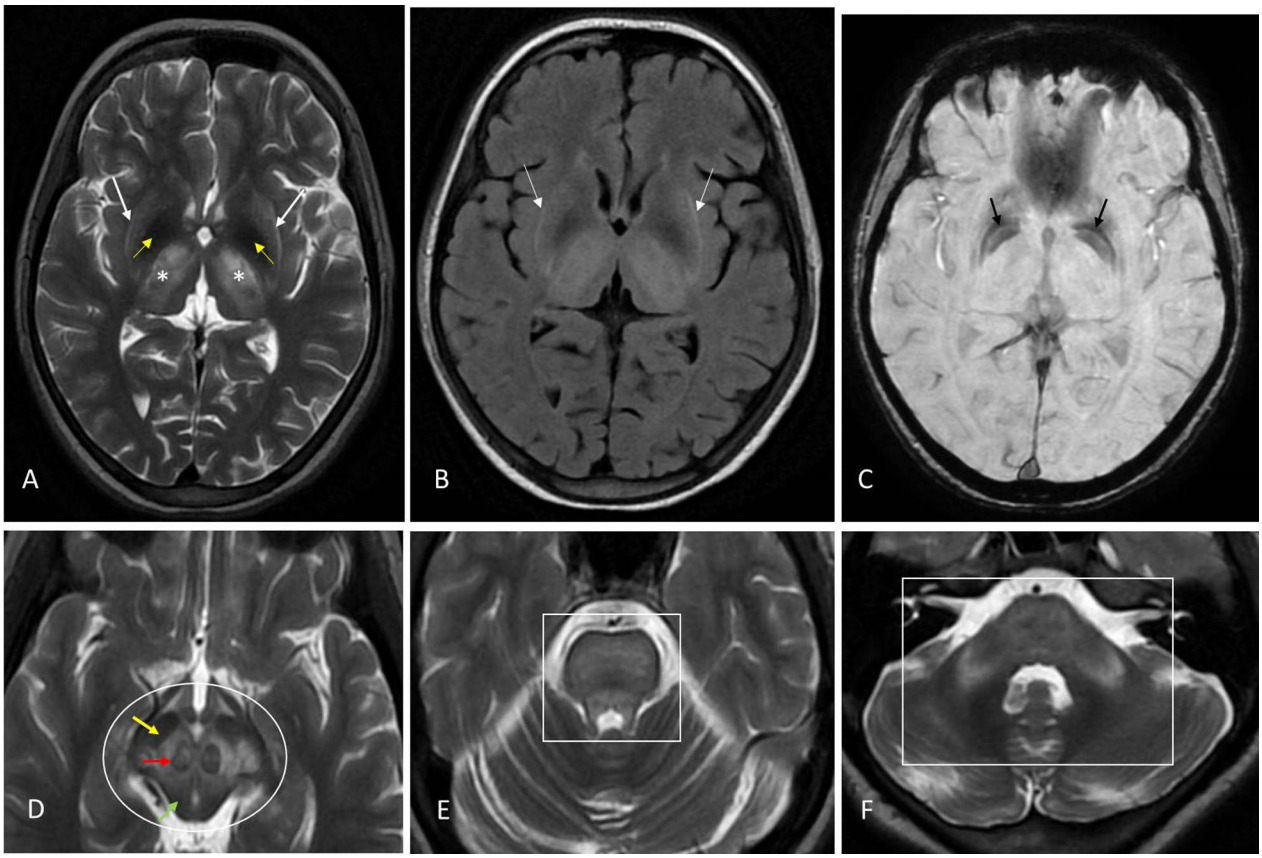

Fig. 4 Axial T2 weighted MR image (**A**) and axial FLAIR MR image (**B**) shows symmetrical hyperintensity in bilateral putamen with thin T2 hyperintensity in claustrum (bright claustrum sign, white arrows in **A** and B) and bilateral thalami (white asterisks). Symmetrical hypointensity is noted in bilateral globus pallidi (yellow arrows). Axial SWAN MR image (**C**) shows symmetrical areas of blooming in bilateral globus pallidi (black arrows). Axial T2 weighted MR image at the level of midbrain (**D**) shows hyperintense tegmentum with hypointense red nuclei (eyes; red arrow), hypointense superior colliculi (chin; green arrow) and pars reticulata of substantia nigra (ears; yellow thick arrow), depicting "face of giant panda sign" (white oval). Axial T2 weighted MR image at the level of pons (**E**) shows hyperintense dorsal tegmentum with hypointense medial longitudinal fasciculus and central tegmental tract (eyes), hyperintense aqueduct opening into fourth ventricle (nose and mouth) and hyperintense superior cerebellar peduncles (cheeks), depicting "face of miniature panda sign" (white box). Axial T2 weighted MR image at the level of middle cerebellar peduncle (**F**) shows symmetrical hyperintensity in bilateral middle cerebellar peduncles (depicted by white box)

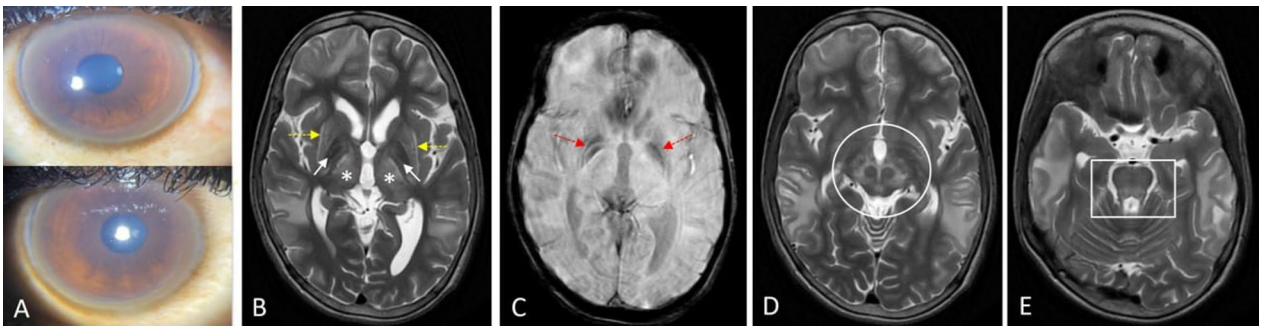

Fig. 5 Slit lamp examination of both eyes showing bilateral Kayser-Fleisher rings (**A**). Axial T2 weighted MR image (**B**) shows symmetrical hyperintensity in bilateral caudate, putamen, posterior limb of internal capsule, bilateral thalami (white asterisks) and bright claustrum sign (yellow arrows). Symmetrical hypointensity is noted in bilateral globus pallidi (white arrows). Axial SWAN MR image (**C**) shows symmetrical areas of blooming in bilateral globus pallidi (red arrows). Axial T2 weighted MR image at the level of midbrain (**D**) and at the level of pons (**E**) shows "face of giant panda sign" (white circle) and "face of miniature panda sign" (white box) respectively

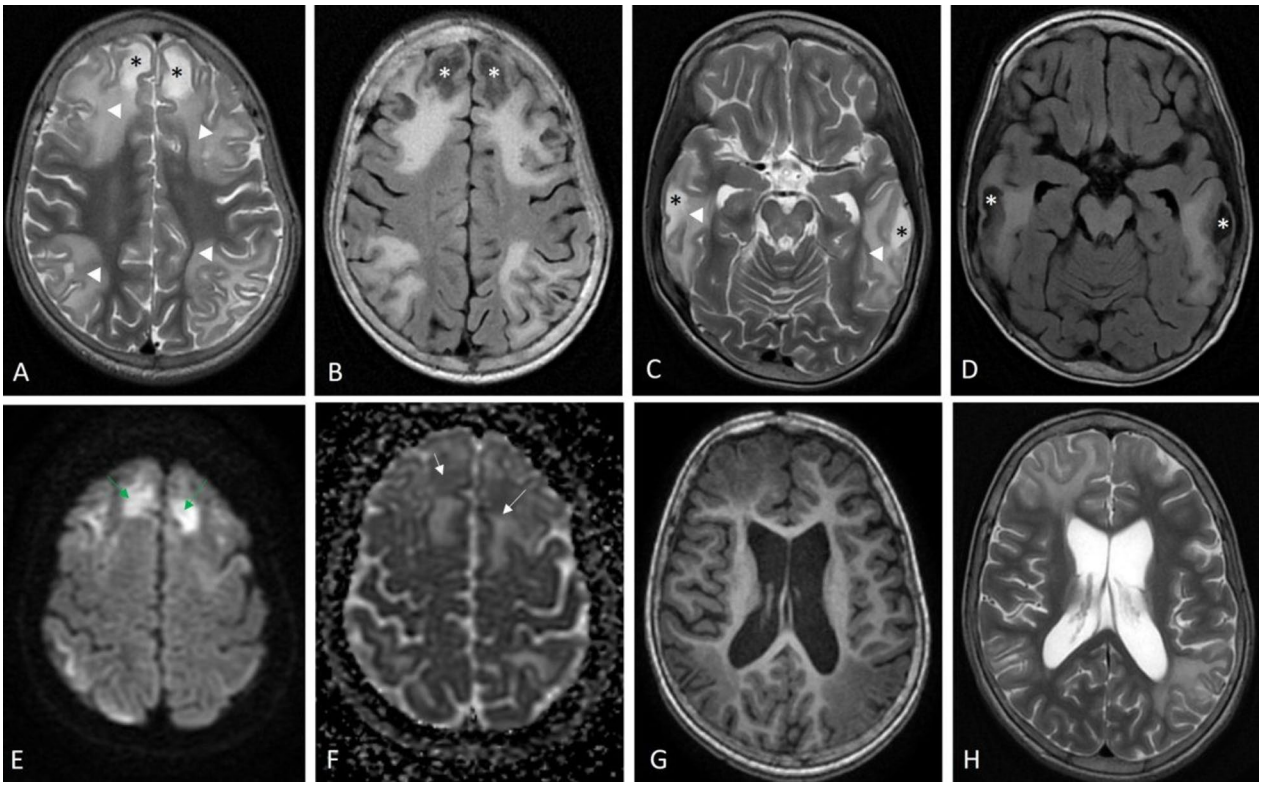

Fig. 6 Axial T2 weighted MR images (**A** and **C**) and axial T2 FLAIR MR images (**B** and **D**) show bilateral, symmetrical, confluent white matter hyperintensities in the frontal, parietal and temporal lobes (white arrow heads). Symmetrical T2 hyperintense (black asterisks) and T2 FLAIR hypointense (white asterisks) subcortical cystic areas seen in bilateral frontal and temporal lobes. Axial b-1000 DWI image (**E**) and corresponding ADC map (**F**) shows focal areas of diffusion restriction in bilateral frontal white matter. Axial T1 weighted and T2 weighted MR images at the level of lateral ventricles (**G** and **H**) show cerebral atrophy in the form of mildly prominent bilateral lateral ventricles

as in all of our patients [4]. Toxic brain injury primarily involves the basal ganglia, and nearly all patients with neurologic involvement develop green to brownish eye lesions called Kayser–Fleischer rings, representing copper deposits in the descemet's membrane of corneal limbus. Wison's disease is diagnosed biochemically by the presence of decreased serum ceruloplasmin, increased hepatic copper content (most sensitive and accurate test), and increased urinary excretion of copper (most specific test) [3].

Radiological imaging with Brain Computed Tomography (CT) markedly under-evaluates the true structural involvement in WD, except for the advanced cases where diffuse brain atrophy or striatal or thalamic hypodensities may be depicted [5]. MRI brain plays an essential role in early diagnosis of Neuro-Wilson's. T1 weighted imaging (T1WI) shows variable signal intensities, with T1 basal ganglia hyperintensity usually representing hepatic involvement of WD [6]. The most common MRI features of WD are bilaterally symmetrical T2/FLAIR hyperintensities in the basal ganglia (putamina, caudate nuclei, globus pallidi), ventrolateral thalami and brainstem (particularly midbrain, with uncommon involvement of pons and medulla) [7, 8]. Kim et al. [6] postulated high signal intensities on T2WI of gray matter nuclei could be explained either by edema, necrosis, gliosis and or cystic degeneration and often represent the cerebral involvement of WD. Often, a thin rim of T2 hyperintensity is seen in the claustrum, designated as the "bright claustrum sign" [9]. At times, T2 Weighted images (T2WI) may depict central hypointensity surrounded by peripheral hyperintensity in the caudate, globus pallidus and putamen [6]. Also, very dark T2 signal intensity may be observed in globus pallidi, reflecting paramagnetic effect of excess iron deposition in addition to the copper in WD [6]. Susceptibility Weighted Imaging (SWI) with T2* (GRE) sequences frequently depict blooming in putamina, caudate nuclei, ventrolateral thalami, and dentate nuclei [6].

The brainstem involvement in the midbrain with characteristic "Face of giant panda sign", on T2WI, is, due to hyperintensity in tegmentum with sparing of red nucleus forming 'eyes, preservation of signal intensity in lateral part of pars reticulata of substantia nigra forming

'ears' and hypointensity in superior colliculus forming 'mouth'[9]. Another classical brainstem sign involving the dorsal pontine tegmentum, is "face of the miniature panda", constituted by hypointensity of medial longitudinal fasciculi and central tegmental tracts ("eyes"), relative to hyperintensity of the aqueduct opening into fourth ventricle ("nose and mouth") and panda's "cheeks" depicted by the hyperintense superior cerebellar peduncles [9–12].

Rare findings like restricted diffusion in corpus striatum on Diffusion Weighted Imaging (DWI) have been described in the early stages of WD. Other uncommon findings like focal or diffuse confluent hyperintensities and atrophic changes with ventricular dilatation may be seen in cerebral and cerebellar hemispheres. Further, cerebellar involvement of dentate nuclei and superior cerebellar peduncles, though, have been published in quite a number of cases in the neuropathologic literature, profound cerebellar involvement on MRI have only seldom been seen [13]. Moreover, to the best of our knowledge, striking abnormal hyperintensity within the middle cerebellar peduncles on MRI as described by King et al. [13] has been very rarely reported in the past.

Additionally, white-matter changes/leukoencephalopathy may be observed in up to 25% of WD patients, atypically, seen as focal or multifocal, symmetrical, T2 weighted hyperintensities, with preferential involvement of frontal lobes [14]. These changes may be explicated by softening, spongy formation, demyelination, and or cavitatory breakdown. Few authors [15, 16] have reported these extensive white-matter changes with subcortical white matter cysts as indicators of longstanding or severe disease, showing rapid progression and neurological deterioration. Conversely, few other authors [17] found leukoencephalopathy even in early course of WD, within 6 months, similar to our case, where the patient showed extensive bilaterally symmetrical white matter hyperintensities in frontal, temporal and parietal lobes with subcortical cysts and patchy diffusion restriction in frontal lobes, within 3 months of disease onset. Another set of authors [18, 19] have correlated white matter changes to post-treatment sequel, following D-penicillamine treatment, a marker of poor response to chelation therapy and subsequent poor outcome. Various Differentials to be thought of in presence of such white matter changes are: acute disseminated encephalomyelitis (ADEM), HIV encephalopathy, and post-hypoxic encephalopathy. However, all of these diagnoses were ruled out in our patient by pertinent history and investigations.

Summarizing the imaging findings in our series of patients: All four patients showed bilateral T2 hyperintensity in putamina and thalami. One of these patients showed peripheral T2 hyperintensity with central hypointensity in bilateral putamina (Fig. 2), as opposed to other three patients which showed complete T2 hyperintensity of bilateral putamina. Three out of four patients showed symmetrical T2 hyperintensity in bilateral caudate nuclei. All four patients showed T2 hypointensity of bilateral globus pallidi with blooming on SWI. Two out of four patients showed bright claustrum sign. Three out of four patients showed brainstem involvement with face of giant panda and face of miniature panda signs. One patient showed features of mild cerebral atrophy, prominent bilateral lateral ventricles, with extensive white matter changes and subcortical cysts. One patient showed conspicuous involvement of bilateral middle cerebellar peduncles.

There are various imaging features of Wilson's disease on MRI, both typical and atypical. Typical features include symmetrical T2 hyperintensity in caudate, putamina, thalami, T2 hypointensity of globus pallidus, bright claustrum sign, brain stem involvement like face of giant panda sign and face of miniature panda sign. While atypical features encompass cerebral as well as cerebellar atrophy, white matter changes, subcortical cysts and hyperintensity of middle cerebellar peduncle. The most common imaging feature encountered in our case series is bilateral T2 hyperintensity in putamina and thalami and T2 hypointensity of bilateral globus pallidi with blooming on SWI followed by T2 hyperintensity in caudate nuclei and brainstem involvement. Patients with typical MRI features showed good response to treatment, On the other hand patients with atypical features showed poor response to treatment with no clinical improvement.

Wilsons's disease is potentially lethal if not treated adequately, with known rapid progression to death. However, with the currently available chelating drugs like Zinc, penicillamine, Trientene and tetrathiomolybdate, initiating an early treatment has shown to reverse the neurological and hepatic manifestations [20].

Conclusions

Wilson's disease is an uncommon disease with varied presentations. MRI plays an indispensible role in adequate evaluation and prognostication of such patients with neuropsychiatric symptoms. Having knowledge about the unusual and atypical imaging features like white matter changes with cysts, middle cerebellar peduncle involvement, over and above the well-known basal ganglia and brainstem features, aid in expediting the diagnosis and consequent treatment. Likewise, radiologists should keep WD as a differential in young patients having progressive neurological disease and MRI showing leukoencephalopathy, thereby contributing to early initiation of treatment and altering the outcome.

Abbreviations

BD	Bis in die (twice a day)
CT	Computed tomography
DWI	Diffusion weighted imaging
FLAIR	Flair attenuated inversion recovery
GRE	Gradient echo sequence
KF	Kayser–Fleischer
MRI	Magnetic resonance imaging
SWI	Susceptibility weighted imaging
TDS	Three times a day
T1WI	T1 Weighted imaging
T2WI	T2 Weighted images
WD	Wilson's disease

Acknowledgements
Not applicable.

Author contributions
Dr AB, Dr KP prepared the initial draft, edited and formatted the draft. Dr AB, Dr KP and Dr NB contributed in relevant data collection of cases. DR AM finally edited the manuscript. 'All authors have read and approved the final manuscript'.

Funding
No funding was obtained for this study.

Availability of data and materials
The content of the manuscript has not been published, or submitted for publication elsewhere.

Declarations

Ethics approval and consent to participate
Patient consent was taken. Ethical approval not applicable.

Consent for publication
Obtained from the patients and parents wherever applicable.

Competing interests
The authors declares that they have no competing interest.

Received: 11 March 2024 Accepted: 2 August 2024
Published online: 12 August 2024

References

1. Shribman S, Bocchetta M, Sudre CH, Acosta-Cabronero J, Burrows M, Cook P et al (2022) Neuroimaging correlates of brain injury in Wilson's disease: a multimodal, whole-brain MRI study. Brain 145:263–275
2. Klatt EC, Kuman V (2020) Robins and cotran atlas of pathology and robbins basic pathology, 10th edn. England, London, pp 849–850
3. Kasper D, Fauci A, Hauser S, Longo D, Jameson JL, Loscalzo J (2019) Harrison's manual of medicine. 20th ed. Columbus. 2982–2984
4. Dev S, Kruse RL, Hamilton JP, Lutsenko S (2022) Wilson disease: update on pathophysiology and treatment. Front Cell Dev Biol 10:871877
5. Osborn AG (2012) Osborn's brain: imaging, pathology, and anatomy. 2nd ed. Salt Lake City, p 989–90.
6. Kim TJ, Kim IO, Kim WS, Cheon JE, Moon SG, Kwon JW et al (2006) MR imaging of the brain in Wilson disease of childhood: findings before and after treatment with clinical correlation. AJNR Am J Neuroradiol 27:1373–1378
7. Zhong W, Huang Z, Tang X (2019) A study of brain MRI characteristics and clinical features in 76 cases of Wilson's disease. J Clin Neurosci 59:167–174
8. Yu X-E, Gao S, Yang R-M, Han Y-Z (2019) MR imaging of the brain in neurologic Wilson disease. AJNR Am J Neuroradiol 40:178–183
9. Panda AK (2013) Classic neuroimaging, the bird's eye view in Wilson's disease. BMJ Case Rep. https://doi.org/10.1136/bcr-2013-200701
10. Gupta A, Chakravarthi S, Goyal MK (2014) "Face of giant panda": a rare imaging sign in Wilson's disease. QJM 107:579
11. Thapa R, Ghosh A (2008) 'Face of the giant panda' sign in Wilson disease. Pediatr Radiol 38:1355
12. Singh P, Ahluwalia A, Saggar K, Grewal CS (2011) Wilson's disease: MRI features. J Pediatr Neurosci 6:27–28
13. King AD, Walshe JM, Kendall BE, Chinn RJ, Paley MN, Wilkinson ID et al (1996) Cranial MR imaging in Wilson's disease. AJR Am J Roentgenol 167:1579–1584
14. Mukherjee S, Solanki B, Guha G, Saha SP (2016) White matter changes in Wilson's disease: a radiological enigma. J Neurosci Rural Pract 7:447–449
15. Sankhyan N, Sharma S, Kalra V, Garg A, Balkrishnan P (2008) Cystic white-matter changes in childhood Wilson's disease. Pediatr Neurol 39:281–282
16. Yu M, Ren L, Zheng M, Hong M, Wei Z (2022) Delayed diagnosis of Wilson's Disease report from 179 newly diagnosed cases in China. Front Neurol 13:884840
17. Wang A, Wei T, Wu H, Yang Y, Ding Y, Wang Y et al (2023) Lesions in white matter in Wilson's disease and correlation with clinical characteristics. Can J Neurol Sci 50:710–718
18. Verma A, Singh NN, Misra S (2004) Early white matter changes in Wilson disease. J Assoc Physicians India 52:578–579
19. Aikath D, Gupta A, Chattopadhyay I, Hashmi MA, Gangopadhyay PK, Das SK et al (2006) Subcortical white matter abnormalities related to drug resistance in Wilson disease. Neurology 67:878–880
20. Bhattacharya K, Thankappan B (2022) Wilson's disease update: an Indian perspective. Ann Indian Acad Neurol 25:43–53

Publisher's Note